energies

Article

Modeling the Effect of Dust and Wind Speed on Solar Panel Performance in Iraq

Israa Amer Dahham [1], Muhammad Ammirul Atiqi Mohd Zainuri [1,2,*], Ali Abdulabbas Abdullah [2] and Mohd Faizal Fauzan [3]

[1] Department of Electrical, Electronic and Systems Engineering, Faculty of Engineering and Built Environment, Universiti Kebangsaan Malaysia (UKM), Bangi 43600, Selangor, Malaysia
[2] Solar Energy Research Institute, Universiti Kebangsaan Malaysia (UKM), Bangi 43600, Selangor, Malaysia; prof.dr.albakry@atu.edu.iq
[3] Al Najaf Technical Collage, Al Furat Al Awsat Technical University, Babylon-Najaf Street, Najaf 54003, Iraq; drfaizalfauzan@ukm.edu.my
* Correspondence: ammirrulatiqi@ukm.edu.my

Abstract: Dust accumulation on a PV panel surface can considerably lead to photovoltaic energy degradation. A particle-based dust accumulation model was proposed to estimate the surface dust coverage fraction on a PV panel. The model determines the effect of the surface dust coverage fraction on the performance of the PV panel. Gravity, wind, and particle-surface interaction forces were resolved to their components, and force balance was established to determine surface-parallel (slipping force) and surface-orthogonal (adhering force) component forces. The proposed model was validated through a schedule of lab and field experiments and by comparing the predicted values with the results of a validated model developed by Lu and Hajimirza. The relationship between a solar panel's output power and the surface dust coverage fraction under the wind effect was established for three types of dust (graphene, silica, and natural dust) using Response Surface Methodology (RSM). Statistical analysis was applied to determine the most and least influencing variables on the output power of three types of solar panels (mono-crystalline, polycrystalline, and thin-film PV panels) exposed to dust accumulation. The obtained results show that dust particle size, wind velocity, and PV panel tilt angle play important roles in enhancing or degrading PV performance. Lower values of the tilt angle resulted in maximum output power, while high values of the tilt angle reduced the incident sunlight on the surface of the PV panel, resulting in lower output power. However, higher values of the tilt angle led to a lower dust coverage area of the PV panel and consequently decreased the power losses of the PV panel. The results also show that wind velocity has a considerable impact on the dust scraping of fine particles from a PV surface. The enhancement percentages of PV performance due to wind influence are 4.85%, 5.85%, and 10.9% for graphene, silica, and natural dust, respectively.

Keywords: photovoltaic panel performance; dust accumulation; gravity; wind effect; tilt angle

Citation: Amer Dahham, I.; Mohd Zainuri, M.A.A.; Abdullah, A.A.; Fauzan, M.F. Modeling the Effect of Dust and Wind Speed on Solar Panel Performance in Iraq. *Energies* **2023**, *16*, 6397. https://doi.org/10.3390/en16176397

Academic Editors: Davide Astolfi and Abu-Siada Ahmed

Received: 30 June 2023
Revised: 18 August 2023
Accepted: 29 August 2023
Published: 4 September 2023

1. Introduction

Solar systems mainly convert optical energy (sun irradiance) into electrical energy. The performance of the PV modules depends on deterministic and stochastic parameters. The deterministic factors are mainly related to the PV cell design factors, such as the material of construction and design. The stochastic factors consist of environmental parameters such as temperature, wind, humidity, dust, and rain [1,2] Dust accumulation on a PV module surface is considered the most deteriorating environmental factor for PV performance [3]. Dust absorbs a significant portion of the irradiance and consequently reduces the conversion of the photo (optical) energy to electrical energy, resulting in lower solar cell efficiency. The adverse impact of the dust on the performance of the PV cell has been extensively investigated by many researchers [4–8]. Also, many cleaning mechanisms were proposed and investigated, such as mechanical vibration mechanisms and charge-induced mechanisms [9–12]. The angle of the incident light plays a major role in increasing or decreasing the optical energy conversion to electrical energy. The best angle of inclination for the PV module to obtain maximum optical energy conversion to electrical energy is when the PV module is orthogonal to the incident light. However, the incident sunlight is highly dependent on the geographic location, and the tilt angle of the solar panel is accordingly manipulated [13]. The geographical location of Iraq near the equator can provide 6.5–7 kw-hr per square meter [13]. Iraq also receives 2800–3300 sunshine hours per year [14]. The tilt angle of the PV module strongly impacts the dust accumulation on the surface of the PV panel. The lower the inclination angle, the higher the dust accumulation, and vice versa [15,16]. Lu and Hajimirza [17] proposed a model that exploits the gravity force as a self-cleaning mechanism for the tilted surface. Their model is based on a monolayer of dust with an adsorption/desorption mechanism, in which a first-order differential equation was developed with two main parameters: adsorption rate and desorption rate. The model also included the interaction forces between the dust particles and the panel surface. However, their model disregarded the effect of wind and soiling effects on the dust coverage fraction. GOOSSENS et al. [18] studied the effect of wind velocity on dust accumulation and PV module power drop and concluded that wind speed is a key factor in airborne dust concentration on the PV module surface and consequently on the drop of power. Picotti et al. [19] related the wind velocity with the soiling phenomenon through four stages of dust particles effects on PV panels: dust generation, dust deposition, dust adhesion, and dust removal. Gholami et al. [20], Mekhilef et al. [21], and Hee et al. [22] had experimentally explored the impact of the wind speed on the dust accumulation of the PV panel. Jiang et al. [23] and Tominaga et al. [24] modeled both dust particle deposition and particle resuspension to predict the dust accumulated over a PV panel under the wind effect. In the early 1950s, many models based on indoor air turbulent flow were developed [25]. However, authors have found that large particles of dust could be efficiently removed by the wind compared to fine particles. The range of diameters of the modeled dust particles is between 0.1 and 100 µm. It was concluded that dust could be partially removed with optimal positioning of a solar cell surface with respect to sunlight direction. Unfortunately, none of the aforementioned studies related the effect of both wind velocity and tilt angle on the dust accumulation over a PV panel. The available literature contains three types of models for estimating the effect of dust accumulation on the performance of PV modules. The first type of model concentrates on dust particle properties (diameter, mass, and density) and uses the particle geometric parameters to estimate the effect of the accumulated dust on the performance of the PV module [26–30]. The second type of model focuses on wind and humidity [31]. The third type of model relates the geometric parameters of the dust particles with air flow and their interactions with the surface of the PV panels [32–35]. To the best knowledge of the authors, none of the three models related the surface dust coverage fraction with either the dust particle's characteristics or wind velocity. The surface dust coverage fraction is strongly dependent on the tilt angle of the PV panel; therefore, the proposed model indirectly investigates the effect of the tilt angle and the wind velocity on the deposition and resuspension of the dust particles. The proposed model successfully calculates the force balance over a dust particle attached to the surface of a PV panel. Gravity and wind (aerodynamic) forces govern the dust particle movement over the surface of the PV panel. The interaction of the dust particle with the surface of the PV panel was also included in the model through Van der Waals and electrostatic forces. The model provides a novel approach to calculate the performance reduction of a PV panel as a function of tilt angle and wind velocity.

The proposed model relates the time evolution of the surface dust coverage fraction of a PV panel to tilt angle. It calculates the reduction of the voltage, current, and power of solar modules due to light hindering by the accumulated dust on the surface of the PV panel. The model, which is presented in Section 2, was divided into three subsections. Sections 2.1 and 2.2 describe and calculate the force balance over a single dust particle resting on the surface of a tilted PV panel. The gravity force and the aerodynamic force that are exerted on the dust particle were analyzed into surface-parallel and surface-perpendicular force components depending on the tilt angle, wind velocity, and particle diameter. The resultant force of the two force components determines whether the gravity force drags the particle downward or sticks the particle to the surface. The total resultant force is the vector summation of the gravity and aerodynamic forces components. The total resultant force is responsible for the dust particles accumulation rate and quantity. The third and last subsection deals with the solar irradiance and the relation between the incident angle of the light and the tilt angle of the PV panel. The optical absorption efficiency of a PV panel is strongly dependent on the dust coverage fraction, light incident angle, and PV panel angle of inclination.

The proposed model indirectly calculates the efficiency of a solar panel when exposed to dust accumulation. The accumulated dust absorbs and reflects part of the incident light, deteriorating the performance of the PV panel. The deterioration was expressed as a surface dust coverage fraction of the PV panel, with dust resulting in lower electrical energy.

Section 2 describes the proposed model and the steps that were followed to derive the model. The section summarizes the theory and the assumptions that facilitate the calculations of the influencing forces and the resultant force. The model also included the relation between the solar absorbed energy and the light incident angle.

Section 3 explained the validation process of the proposed model, statistically analyzed it, and discussed the obtained results. The obtained results reflected the strong dependence of the PV performance on the tilt angle and the wind velocity. The results are expressed in the form of tables and figures to provide better visualization of the effect of the most and least influencing parameters.

Section 4 summarizes the conclusions and recommendations for the present research.

2. Model Description

The model is divided into two main parts: the dust particle accumulation mechanism over the surface of a PV module, and the sunlight incident angle effect on the performance of a PV module.

2.1. Dust Accumulation over the Surface of a Tilted PV Panel

The model is based on the following assumptions:

- Dust particles accumulate on the surface of PV panels in monolayer form. Dust particles do not form multilayers, as particles cannot accumulate on top of each other due to the instability of the upper dust layers. Therefore, the monolayer is formed through the interaction between the dust particles and the surface of the PV panels. The forces that are responsible for the adhesion of the dust particles to the surface of PV panels are Van der Waals and electrostatic forces. The Van der Waals force is a distance-dependent interaction force between particles [36], while the electrostatic force is an electric-field-induced attraction force of dust particles onto the surface of PV panels [37]. This assumption explains that the optical impact of a single particle on the PV yield is a material property, i.e., how much light is absorbed by the particle and how much light is transmitted through the particle to the surface of the PV panels. The optical impact of a monolayer of dust particles on the PV yield is strongly dependent on material properties and layer thickness, which reduce the light that arrives at the PV module.
- Attachment and detachment of dust particles on the surface of a PV panel are governed by gravity forces, interparticle forces (Van der Waals and electrostatic forces), and aerodynamic forces (lift and drag) which are induced by wind velocity. Dust particles that accumulate on the surface are uniformly distributed in a monolayer. If extra dust particles accumulate to form a top layer, the particles are likely to detach due to the lift force induced by wind. Therefore, the effect of dust particles on the PV yield depends on the optical properties of the particles and the thickness of the formed layer.

The weight of the particle (gravity force) shown in Figure 1 was resolved into two force components: the surface-parallel force component (F_S) and the surface-orthogonal force component (F_R). The surface-parallel force tries to slip the dust particle downward (slipping force), while the surface-orthogonal force tries to adhere the dust particle to the panel surface (resisting force).

$$F_1 = F_s = mg\,sin\,\beta \quad (1)$$

$$F_2 = F_R = mg\,cos\,\beta + F_{vander} + F_{electrocstatic} \quad (2)$$

where m is the mass of particle, g is the gravitational force, β is the tilt angle, F_{vander} is the Van der Waals force, and $F_{electrostatic}$ is the electrostatic force. Equation (2) includes interparticle forces: Van der Waals force (F_{vander}), and electrostatic forces ($F_{electrostatic}$). These interparticle forces represent cohesive forces between adjacent particles.

$$F_{vander} = \frac{h_w d}{8\pi z_0^2} \quad (3)$$

$$F_{electrostatic} = F_{eli} + F_{eld} + F_{elf} \quad (4)$$

where F_{eli} is the electrostatic image force, F_{eld} is the electrostatic double layer force, F_{elf} is the electrostatic field force, h_w is the Lifshitz constant, d is the diameter of the particle, and z_0 is average distance between the dust particle and the solar panel.

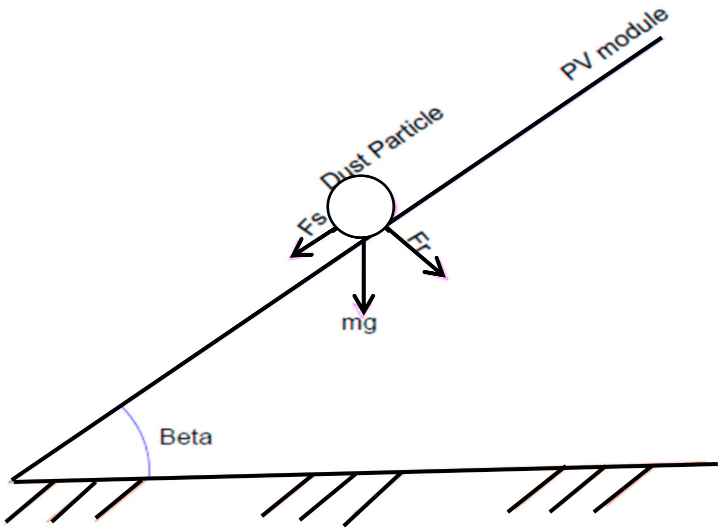

Figure 1. Dust particle rests on a tilted PV panel under the gravity force effect.

Then, substituting for F_{vander} and $F_{electrostatic}$, Equation (2) becomes the following:

$$F_R = mg\,cos\,\beta + \frac{h_w r_d}{8\pi z_0^2} + F_{eli} + F_{eld} + F_{elf} \quad (5)$$

Equation (5) calculates the orthogonal force that adheres the dust particle to the surface of the PV panel.

2.2. Dust Accumulation over a Surface of a PV Panel under Wind Force Effect

Dust particles resting on a tilted PV panel surface under the effect of an airstream are exposed to many forces, including the drag force F_d, the lift force F_L, the gravity force F_g, and the interparticle force F_i. The aerodynamic forces F_d and F_L are related to wind shear near the surface and hence are functions of the surface friction velocity u_s. Threshold friction velocity u_{th} is the minimum velocity which is required to induce wind erosion. At

$u_s = u_{th}$, the aerodynamic forces just overcome the retarding forces F_g and F_i to initialize the movement of soil particles, as shown in Figures 2 and 3.

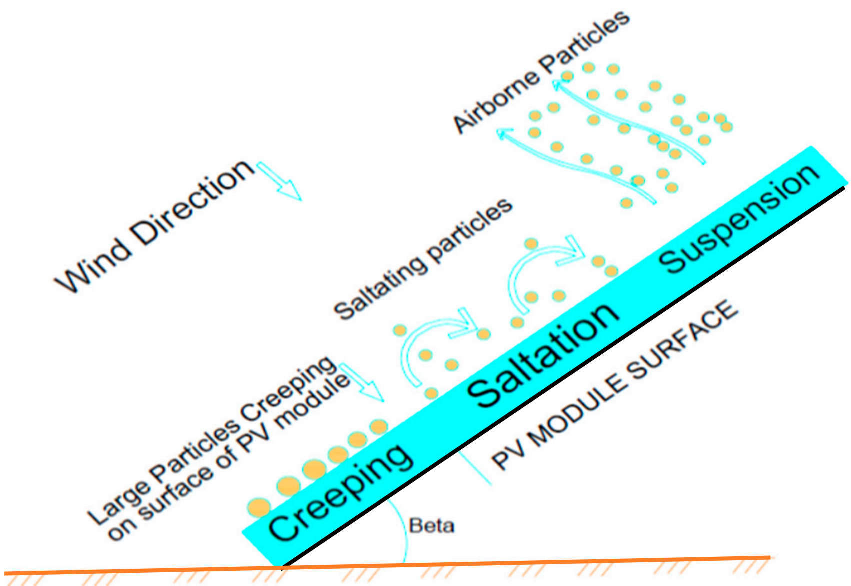

Figure 2. Wind-particle interactions: large particles creep, medium particles saltate, and fine particles suspend. Deduced from [38].

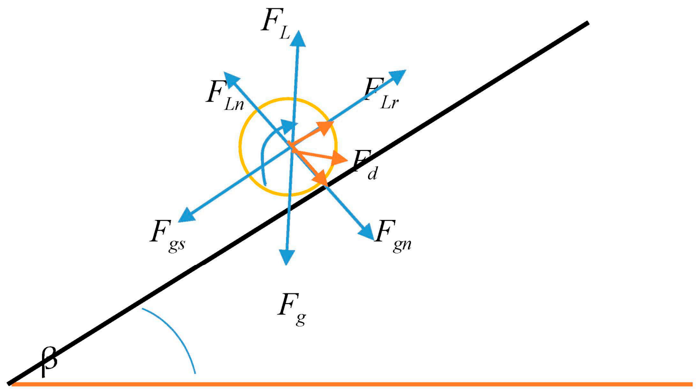

Figure 3. Force balance on a particle resting on a PV panel.

Figure 2 shows that large particles ($\geq$0.5 mm in diameter) are dragged over the surface of the PV module under the effect of gravity, because they are too heavy to be lifted by wind. Particles ranging between 0.1 mm and 0.5 mm in diameter can be lifted for a very short time and then dropped to result in a hop and bounce motion over the surface of the PV module (saltation motion). Particles less than 0.1 mm in diameter suspend under the effect of wind force.

The applied forces on the dust particle are gravity force F_g, which is resolved into the sliding force component F_{gs} and the normal force component F_{gn}, lift force F_L, which is resolved into the retarding force component F_{Lr} and the normal lift component F_{Ln}, and drag force F_d, which is resolved into the retarding force component F_{dr} and the normal force component F_{dn}. The slipping and retarding force resultants are presented in Equations (6)–(9).

$$F_S = F_{gs} - F_{Lr} - F_{dr} \tag{6}$$

$$F_R = F_{gn} + F_{dn} - F_{Ln} + F_{vander} + F_{electrostatic} \tag{7}$$

Equation (6) represents the resultant of the surface parallel forces that drag the dust particle downward. Equation (7) demonstrates the resultant of the surface parallel forces, which prevent the dust particle from slipping downwards.

Substituting for forces in Equations (6) and (7) with their equivalents yields, as follows:

$$F_S = mg\,sin\beta - k_l\rho d^2 u_s^2 sin\,\beta - k_d\rho d^2 u_s^2 sin\,\beta \tag{8}$$

$$\begin{aligned} F_R = mg\,cos\,\beta + k_d\rho d^2 u_s^2\,cos\,\beta - k_l\rho d^2 u_s^2\,cos\,\beta + \tfrac{h_w d}{8\pi z_0^2} + \tfrac{Q_{dust}^2}{4E(d+z_0)^2} \\ + \tfrac{\pi E U^2 d}{2z_0} + \tfrac{\sigma Q_{dust}}{E} \end{aligned} \tag{9}$$

where m is the mass of the dust particle, g is the gravitational force, ρ is the dust density, d is the particle diameter, u_s is the surface friction velocity, k_d is the drag coefficient, β is the tilt angle, k_i is the lift coefficient, h_w is the Lifshitz constant, z_0 is the average distance between dust particle and solar panel, Q_{dust} is the particle charge, E is the permittivity of free space, and U is the contact potential difference. Table 1 shows the values and units of each constants and parameter used.

Table 1. Values and units of the constants and parameters used in the model.

Parameter	Value	Units	Reference
Gravity acceleration, g	9.81	m/s^2	---
Lifshitz constant, h_w	2.3	ev	Rentsch et al. [39] Meng et al. [40]
Particle density, ρ	1600	Kg/m^3	---
Average distance, z_0	2.343×10^{-8}	m	Meng et al. [40]
Particle charge, Q_{dust}	5.86×10^{-17}	C	Meng et al. [40]
Free space permittivity, E	8.85×10^{-12}	F/m	Typical value for Permittivity of Free Space
Electrical potential difference, U	0.1	V	Meng et al. [40] Usually assigned 0.0–0.5 V
Surface charge density, σ	0.32×10^{-6}	C/m^2	Behrens et al. [41]
Drag coefficient k_d	0.1	...	Liu et al. [42]
Lift coefficient k_l	0.5	...	Ekanayake et al. [43]

Substituting constants and steady-state parameters in Equations (8) and (9), we obtain the following:

$$F_S = 13341.6xd^3\,sin\,\beta - 0.0169d^2W^2\,sin\,\beta \tag{10}$$

$$\begin{aligned} F_R = 13341.6d^3\,cos\,\beta + 7.635 \times 10^{-3}d^2W^2\,cos\,\beta + 2.668 \times 10^{-5}d + \tfrac{9.7\times10^{-23}}{(d+2.343\times10^{-8})^2} + 5.93 \times 10^{-6}d \\ +2.115 \times 10^{-12} \end{aligned} \tag{11}$$

Equations (10) and (11) estimate the slipping and retarding forces (F_s and F_R) of a spherical particle resting on a tilted PV panel surface. Both forces depend on three main parameters: particle diameter (d), wind velocity (W), and tilt angle (β).

Equations (12) and (13) determine the fraction of the panel surface area covered with dust. Therefore, the surface dust coverage fraction (ε) can be modeled as follows:

$$\frac{d\varepsilon}{dt} = F_R(1-\varepsilon) - F_S\cdot\varepsilon \tag{12}$$

Rearranging and integrating Equation (12) yields the following:

$$\varepsilon = \frac{1}{-(F_R + F_S)} e^{-(F_R+F_S)t} - \frac{F_R}{-(F_R + F_S)} \tag{13}$$

The dust surface coverage fraction (ε) represents the fraction of the surface area of the PV panel that is covered with dust. The covered portion of the surface area of the PV panel is determined by the force balance between the slipping force F_s and the retarding force F_R. However, the summation of the covered portion of the surface of the PV panel and the portion of the uncovered surface equals 1, and since F_R is the force that is responsible for the adhesion of dust particles to the surface of the PV panel and F_S is the slipping force. Therefore, the difference between the two forces will determine the uncovered area of the surface of the PV panel covered with dust.

2.3. Solar Irradiance

The amount of solar radiation that is received from the sun is expressed in w/m^2. Spectral irradiance is simply defined as resolving solar irradiance into its principal wavelengths of light. The study of the sun's irradiance extends over visible light, infrared light (IR), ultraviolet light (UV), and X-ray light. Iraq lies between latitudes 2950–37,220 N and longitudes 38,450–48,450 E, and it has an area of 435,052 km^2. The average annual radiation at the southern sites of Iraq was found to be 7263.97 MJ/m^2. The annual solar irradiance in the Baghdad area is approximately >3000 h. The maximum value of ultraviolet radiation in Baghdad City, Iraq, was found on 13 June to be 50.1 W/m^2 [44]. The interaction between the accumulated dust on the surface of the PV panel and the solar irradiance is strongly dependent on the wavelength of the incident radiation. The wavelengths affect the PV module's performance. It was found that the effect of dust on spectral irradiance at each wavelength caused the photon flux to decrease by a maximum of 3.61% at wavelengths 350–450 nm, which lie within the UV spectrum [45]. Therefore, this research focused on UV sources.

The azimuthal angle of the solar panel was assumed to be zero deviated. To obtain a relationship between the incident angle of the sunlight and both the tilt angle of the panel and the zenith angle, we need to understand the definitions of the incident and zenith angles. The zenith angle is simply defined as the radiation angle in relation to the normal ground surface, while the angle between the normal of the tilted panel and the sunlight is called the incident angle.

The relationship between the solar zenith angle, incident angle, and tilt angle can be expressed using Equation (14).

$$\theta = \phi - \beta \tag{14}$$

where θ is the incident angle, ϕ is the solar zenith angle, and β is the tilt angle.

For a solar irradiance profile, $I_{(\omega)}$ at a wavelength ω, the optical absorption efficiency $F(\theta, \beta)$ of the solar system at the wavelength ω, and the incident angle θ is as follows:

$$F(\theta,\beta) = (1 - (1-\gamma)\frac{1}{-(F_R + F_S)} e^{-(F_R+F_S)t} - \frac{F_R}{-(F_R + F_S)}) \cdot \left(1 - \frac{\int I(\omega)R(\omega,\theta)d\omega}{\int I(\omega)d\omega}\right) \cdot \left(\frac{1 - e^{-cos(\theta)/ar}}{1 - e^{-1/ar}}\right) \tag{15}$$

where γ is the average transmission of a dust layer, $I_{(\omega)}$ is the solar irradiance profile at wavelength ω, $R(\omega, \theta)$ is the reflectance of the solar cell surface at wavelength ω, and ar is the angular loss coefficient, which is assumed constant and equals 0.155. $R(\omega, \theta)$ is the average of reflectivity for s-polarized and p-polarized radiation. Fresnel's equations were used to calculate the s-polarized and p-polarized radiations, as shown in Equation (16).

$$R_S(\omega,\theta) = \left| \frac{n1cos\theta - n2\sqrt{1-(\frac{n1}{n2}sin\theta)^2}}{n1cos\theta + n2\sqrt{1-(\frac{n1}{n2}sin\theta)^2}} \right|^2$$
$$R_P(\omega,\theta) = \left| \frac{n1\sqrt{1-(\frac{n1}{n2}sin\theta)^2} - n2cos\theta}{n1\sqrt{1-(\frac{n1}{n2}sin\theta)^2} + n2cos\theta} \right|^2 \quad (16)$$

where $n1$ is the refractive index of air, which equals 1.0003, $n2 = n_\omega + ik_\omega$ is the complex refractive index of silicon (solar cell) at wavelength ω. n_ω and k_ω are depicted in [15].

Solve Equation (9) and find $R(\omega,\theta)$ as the average of the two values of $R_s(\omega,\theta)$ and $R_p(\omega,\theta)$:

$$R(\omega,\theta) = \frac{R_S(\omega,\theta) + R_P(\omega,\theta)}{2}$$

Substitute $R(\omega,\theta)$ in the equation, then solve as a function of time and the specific value of ω. γ is 0.89 for 10 days of dust accumulation [29].

$$F(\theta,\beta) = (1-(1-\gamma)\cdot\frac{1}{-(F_R+F_S)}e^{-(F_R+F_S)t} - \frac{F_R}{-(F_R+F_S)})\cdot(1-R(\omega,\theta)\cdot\left(\frac{1-e^{-cos(\theta)/ar}}{1-e^{-1/ar}}\right) \quad (17)$$

3. Results and Discussion

Model Validation

The validation of the proposed model has been accomplished by comparing the predicted results of the model with experimental data and other researchers' results. The obtained results of the proposed model and the experimental data were statistically analyzed using the Analysis of Variance (ANOVA) technique to determine how well the proposed model fits the experimental data. The results of the proposed model were also compared to [15] model's results. Both comparisons showed fair agreement between the results of the proposed model, the results of the experiments, and the results of the Lu and Hajimirza model. Table 2 shows the comparison of performance reduction percent between the proposed model and the Lu and Hajimirza model [15].

Table 2. Comparison of performance reduction percent between the proposed model and the Lu and Hajimirza model.

No	Model	Performance Drop (Reduction) Percent
1	Lu and Hahimirza [15]	14%
2	Proposed model (Graphene)	8.15%
3	Proposed model (Silica)	9.15%
4	Proposed model (Natural dust)	3.1%

An extensive schedule of field tests, which were carried out for three types of dust (graphene, silica, and natural dust), were statistically analyzed to obtain Equations (16)–(18). The equations predict the output power of solar panels partially covered with graphene (P_G), silica (P_S), and natural dust (P_{ND}) particles, respectively. A field-scale set-up was used to perform nineteen statistically designed field tests for each type of dust (graphene, silica, and natural dust), as shown in Tables 3–5. The set-up consists of a variable angle panel mounting skid, a digital anemometer type GM8901, an air blower, an interface through an ARDUINO card with a 16 MHZ processor, 2 KB of SRAM and 32 KB of FLASH memory, 14 digital I/O, 6 analog I/O, a voltage sensor, and a current sensor. The relationships between a group of controlled experimental parameters (tilt angle of PV panel, wind velocity, particle diameter, and incident light wavelength) and measured responses (output power) for each type of dust (graphene, silica, and natural dust) were determined via implementing a set of mathematical and statistical techniques established by Response Surface Methodology (RSM) [46,47]. Nineteen statistically designed runs (field tests) were performed for different combinations of PV system parameters (dust particle size, panel tilt angle, wind velocity), for each type of dust (graphene, silica, and natural dust), so as to calculate the PV output power for clean and polluted conditions. The results of the output power are further analyzed using Minitab-17 software, where an empirical relationship between the PV output power and the independent variables was fitted and correlated by Equations (18)–(20). The yield of each type of PV panel was calculated for clean and polluted panels by dividing the obtained output power (KW) by the surface area of the panel (m^2). The PV yield for a clean PV surface was 10.9% based on the manufacturer's datasheet. For polluted and inclined PV panels, the PV yield ranged between 5.3% and 8.5% for graphene-polluted panels. When silica dust was used as a pollutant, the PV yield ranged between 7.5% and 10.3%, while for natural dust, the PV yield ranged between 8.2% and 9.4%.

$$\begin{aligned} P_G = 19.41 &+ 0.2656 d_p - 0.2939\beta - 0.329W - 0.01425\omega - 0.000026 d_p^2 + 0.002294\beta^2 + 0.04W^2 \\ &+ 0.000017\omega^2 - 0.000031 d_p\beta - 0.00015 d_p W \\ &+ 0.000002 d_p\omega + 0.00467\beta W + 0.000028\beta\omega - 0.000438 W\omega \end{aligned} \tag{18}$$

$$\begin{aligned} P_S = 19.28 &+ 0.04384 d_p + 0.1022\beta - 0.452W - 0.0036\omega - 0.000054 d_p^2 - 0.000833\beta^2 - 0.1136W^2 \\ &+ 0.000005\omega^2 - 0.000146 d_p\beta + 0.00005 d_p W \\ &+ 0.000004 d_p\omega + 0.00208\beta W - 0.000111\beta\omega + 0.000719 W\omega \end{aligned} \tag{19}$$

$$\begin{aligned} P_{ND} = 20.00 &+ 0.0075 d_p - 0.1109\beta - 0.21W - 0.00912\omega - 0.000007 d_p^2 + 0.000772\beta^2 - 0.0259W^2 \\ &+ 0.000011\omega^2 - 0.000051 d_p\beta + 0.000031 d_p W \\ &+ 0.000003 d_p\omega + 0.00367\beta W - 0.000035\beta\omega - 0.000025 W\omega \end{aligned} \tag{20}$$

Tables 3–5 demonstrate a comparison between predicted values of the output power of solar panels and the measured powers for graphene, silica, and natural dust, respectively. The R^2 of Tables 3–5, which were obtained from the Analysis of Variance (ANOVA) technique, are 96.77%, 95.52%, and 89.13%, respectively. As the ANOVA technique was followed for statistical analysis, the F-value and p-value were considered to evaluate the scatter of the predicted values. The F-values for the cases are 25.66, 18.27, and 7.02, respectively.

The effect of dust particle size on the coverage fraction of the accumulated dust on surfaces of PV panels was investigated under various tilt angles (30, 45, and 60 degrees) and different wind velocities of 2, 4, and 6 m/s. The results are presented in Figure 4a,b. The dust coverage fraction sharply declines as the dust particle diameter increases from 100 µm to 500 µm, indicating the dominance of the gravity force among the forces acting on the dust particle. A further increase in particle diameter resulted in an inconsiderable decrease in the dust particle fraction of the PV panel. Therefore, dust removal from the surface of PV panels strongly depends on the dust particle size. The wind velocity also exhibited a considerable effect on the small dust particle sizes at relatively high velocities. Equation (13) was applied for three different particle sizes (0.1, 0.5, and 1.0 mm) that simulate the prevailing range of dust particle size in Iraq during the sandstorm season. It was applied at various tilt angles and wind velocities.

Table 3. Comparison between predicted values of the output power of a PV module and the measured values when the PV module surface is partially covered with graphene dust.

Run Order	Dust Particle Diameter (μm)	Tilt Angle of Solar Panel (degrees)	Wind Velocity (m/s)	Incident Light Wavelength (nm)	Measured Electrical Power (watt)	Predicted Electrical Power (watt)	Difference between Pred. and Meas. Values
1	100	30	4	400	10.78	11.49958	6.25%
2	300	60	4	400	13.06	13.29833	1.8%
3	300	45	6	400	14.22	14.16292	−0.4%
4	500	45	4	400	14.51	14.68375	1.2%
5	300	60	6	400	12.63	12.84542	1.6%
6	300	45	4	400	13.01	13.06667	0.43%
7	100	45	2	400	10.07	10.215	1.4%
8	300	30	6	400	14.86	14.56375	−2.0%
9	500	30	4	400	15.01	15.57458	3.6%
10	100	45	4	400	11.01	10.54208	−4.4%
11	300	45	2	400	13.69	13.98792	2.1%
12	500	45	6	400	14.12	14.02833	−0.6%
13	300	60	2	400	12.64	12.64208	0.01%
14	500	45	2	400	14.12	14.225	0.74%
15	300	30	4	400	15.23	15.045	−1.2%
16	100	60	4	400	10.01	9.68625	−3.3%
17	300	30	2	400	15.43	14.92042	−3.4%
18	100	45	6	400	10.31	10.25833	−0.5%
19	500	60	4	400	13.87	13.39125	−3.5%

Table 4. Comparison between predicted values of the output power of a PV module and the measured values when the PV module surface is partially covered with silica dust.

Run Order	Dust Particle Diameter (μm)	Tilt Angle of Solar Panel (degrees)	Wind Velocity (m/s)	Incident Light Wavelength (nm)	Measured Electrical Power (watt)	Predicted Electrical Power (watt)	Difference between Pred. and Meas. Values
1	100	30	4	400	14.66	14.53225	−0.8%
2	300	60	4	400	18.116	17.56975	−3.1%
3	300	45	6	400	17.06	17.34992	1.6%
4	500	45	4	400	16.95	17.23533	1.6%
5	300	60	6	400	16.15	16.35867	1.27%
6	300	45	4	400	18.06	17.85	−1.1%
7	100	45	2	400	13.96	14.05408	0.67%
8	300	30	6	400	17.88	17.81433	−0.37%
9	500	30	4	400	18.67	18.06225	−3.36%
10	100	45	4	400	14.24	14.226	−0.09%
11	300	45	2	400	17.98	17.23892	−4.3%
12	500	45	6	400	16.38	16.46575	0.5%

Table 4. *Cont.*

Run Order	Dust Particle Diameter (μm)	Tilt Angle of Solar Panel (degrees)	Wind Velocity (m/s)	Incident Light Wavelength (nm)	Measured Electrical Power (watt)	Predicted Electrical Power (watt)	Difference between Pred. and Meas. Values
13	300	60	2	400	16.14	16.477	2.0%
14	500	45	2	400	16.38	16.66908	1.7%
15	300	30	4	400	18.07	18.79608	3.8%
16	100	60	4	400	13.67	13.82658	1.1%
17	300	30	2	400	18.12	18.18267	0.34%
18	100	45	6	400	13.88	13.77075	−0.8%
19	500	60	4	400	15.93	15.60658	−2.0%

Table 5. Comparison between predicted values of the output power of a PV module and the measured values when the PV module surface is partially covered with natural dust.

Run Order	Dust Particle Diameter (μm)	Tilt Angle of Solar Panel (degrees)	Wind Velocity (m/s)	Incident Light Wavelength (nm)	Measured Electrical Power (watt)	Predicted Electrical Power (watt)	Difference between Pred. and Meas. Values
1	100	30	4	400	15.45	16.00542	3.47%
2	300	60	4	400	16.01	15.97625	−0.2%
3	300	45	6	400	16.44	16.39875	−0.25%
4	500	45	4	400	16.38	16.635	1.5%
5	300	60	6	400	14.96	15.22	1.7%
6	300	45	4	400	15.94	15.92333	−0.1%
7	100	45	2	400	15.12	15.09792	−0.14%
8	300	30	6	400	16.9	16.67833	−1.3%
9	500	30	4	400	16.89	17.31708	2.4%
10	100	45	4	400	15.65	15.30167	−2.2%
11	300	45	2	400	16.01	16.16042	0.9%
12	500	45	6	400	16.01	16.01625	0.04%
13	300	60	2	400	14.96	15.08833	0.85%
14	500	45	2	400	16.01	16.07958	0.43%
15	300	30	4	400	17.31	17.32792	0.1%
16	100	60	4	400	14.95	14.63208	−2.1%
17	300	30	2	400	17.34	16.98667	−2.0%
18	100	45	6	400	15.07	14.98458	−0.57%
19	500	60	4	400	15.78	15.33375	−2.9%

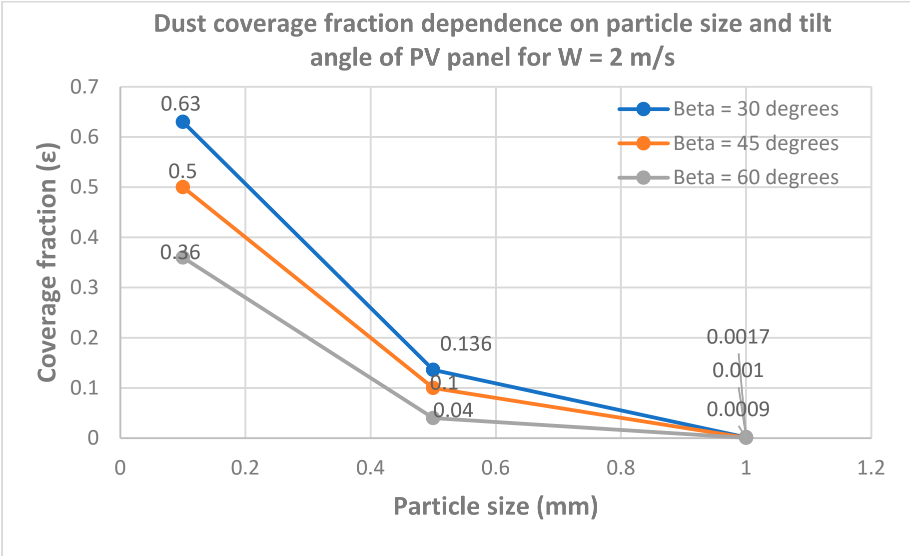

(**a**)

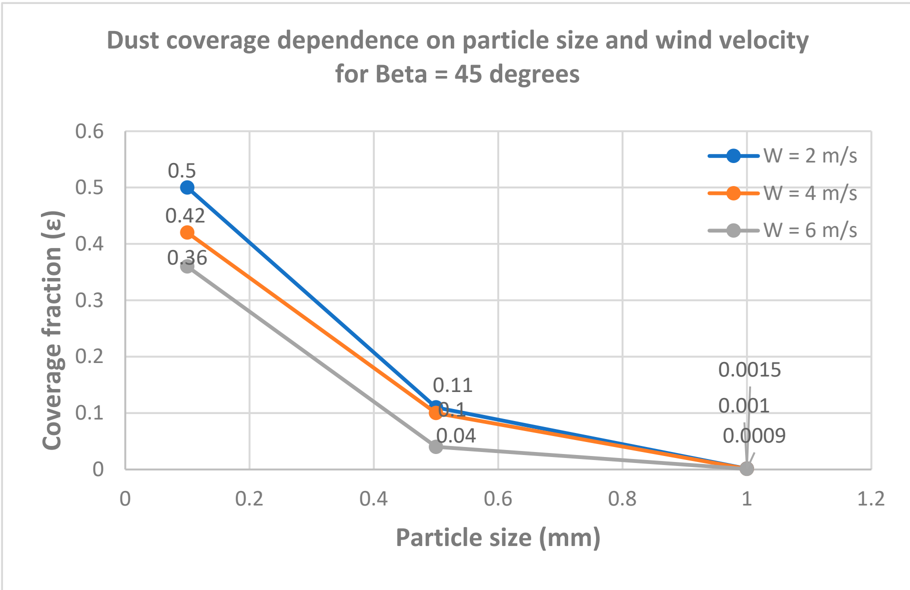

(**b**)

Figure 4. Effect of dust particle size, wind velocity, and tilt angle on the dust coverage fraction over a PV panel: (**a**) effect of tilt angle at wind velocity of 2 m/s, (**b**) effect of wind velocity at tilt angle of 45 degrees.

The effect of the tilt angle of PV panels on the dust coverage fraction is shown in Figure 5. It is clearly seen that increasing tilt angle results in higher removal of dust particles. However, the dust coverage fraction of a PV panel with small dust particles (100 µm) shows a low decline rate with increasing tilt angle. Large dust particle sizes (≥500 µm) show a significant reduction rate in the dust coverage fraction with increasing tilt angle. Particle sizes larger than 500 µm show a limited dust coverage fraction of PV panels, which clearly reflects the self-cleaning mechanism of PV panels under low to high wind velocities. However, small dust particles are strongly affected by wind velocity. Higher wind velocities become the dominant force for the removal of the fine dust particles due to the particle suspension mechanism (lift force). Figure 5 compares the behavior of three dust particle sizes subjected to scraping and lift forces as a function of the tilt angle of PV panels.

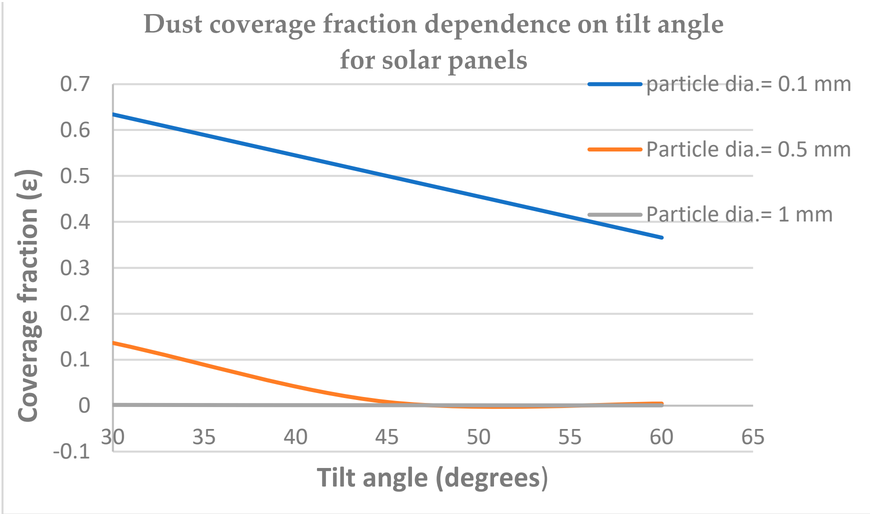

Figure 5. Effect of tilt angle on the dust coverage fraction for different particle sizes.

The effect of three different dust types (graphene, silica, and natural dust) on the output power of PV panels was investigated. The investigations extend over many environmental conditions. The environmental factors that have been studied are wind velocity, particle size, and PV panel tilt angle. The effect of the dust particle size on the output power of the PV panel is presented in Figure 6a–f.

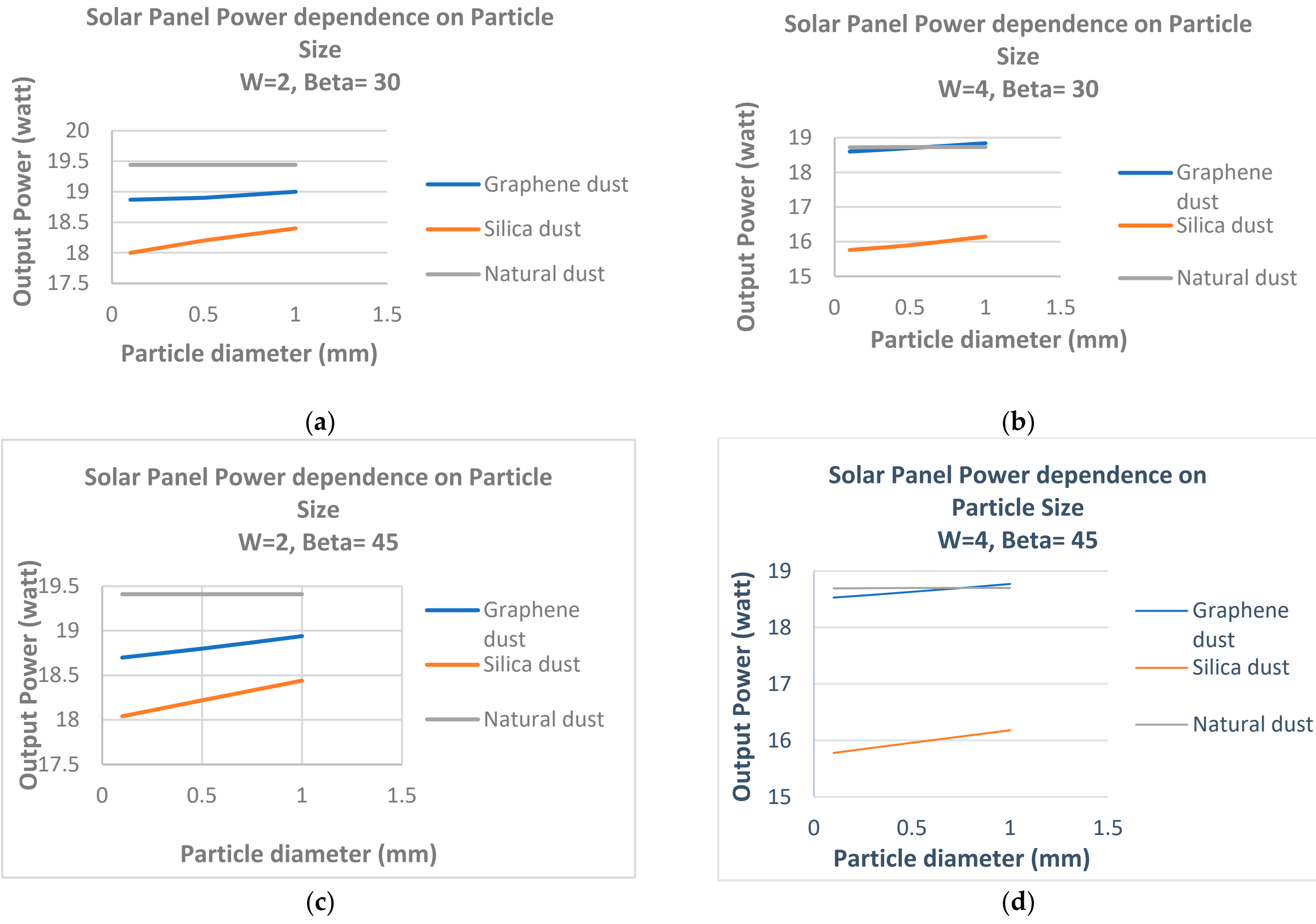

Figure 6. *Cont.*

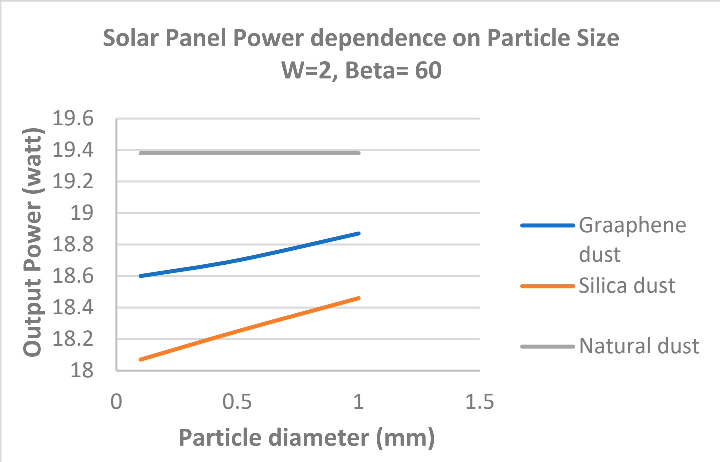

(**e**)

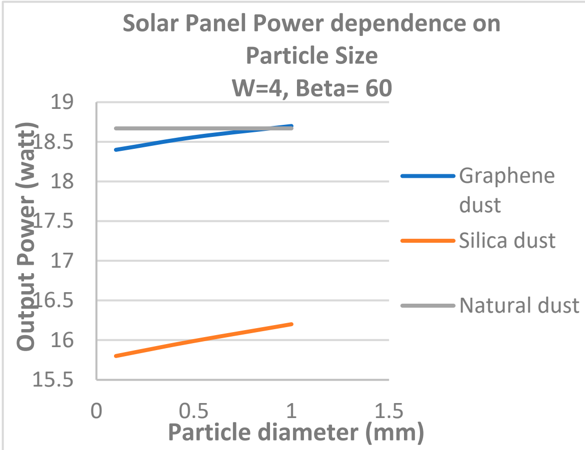

(**f**)

Figure 6. Effect of graphene, silica, and natural dust particle size on the output power of PV modules under various wind velocities and tilt angles. (**a**,**b**) β = 30, W = 2, 4 m/s. (**c**,**d**) β = 45, W = 2, 4 m/s. (**e**,**f**) β = 60, W = 2, 4 m/s.

Figure 6a–f shows that the particle size of the natural dust exhibits an insignificant effect on the PV output power due to the spectrophotometric and crystallographic characteristics of the natural dust. The light absorbance of the natural dust obtained during this course of work was very low, resulting in only a light obscuring effect, which is strongly dependent on the dust accumulation layer. The dust accumulation layer of the natural dust was found to be minimal as it is strongly affected by gravity and wind forces, where large particles are easily slipped downward and small particles are lifted by wind. On the contrary, silica dust particles indicate a considerable effect on the output power of the PV panel. It resulted in the lowest output power of the PV panel when partially accumulated on the surface of the panel. It is attributed to the crystallographic characteristics of the silica, as its hygroscopic properties result in conjoined particles that form a thin layer that obscures light from irradiating PV cells. Graphene dust particles demonstrate a combined effect of spectrophotometric and crystallographic characteristics. Graphene dust particles absorb incident light in the UV spectrum and significantly reduce the conversion of the optical energy into electrical energy.

The effect of wind velocity on the output power of the PV panel is clearly seen in Figure 6a–f. The higher wind velocity induced the movement and saltation of particles of silica and natural dust to form dense dust accumulation layers over the covered area. This dense and opaque layer results in a higher obstruction of sunlight, which was observed to lower the output power of the PV panel. A comparison between Figure 6c,d and Figure 6e,f confirms the main conclusion that silica and natural dust were affected by higher wind velocity, forming dense and opaque layers of accumulated dust. However, it seems that the effect of wind velocity on the amorphous dust particles is more considerable than that on crystalline particles, as higher wind velocity causes amorphous particles to accumulate in a multilayer due to the adhesion capacity of the amorphous materials. The results of the proposed model were compared to the [15] model results. The comparison revealed that the proposed model outperforms the [15] model, as the proposed model resulted in higher output power values of the PV module under the same conditions as the [15] model. The reason behind this difference is attributed to the inclusion of the wind effect besides the gravity force in the proposed model, while the [15] model considers the gravity force as the main force.

4. Conclusions

A particle-based dust accumulation model was proposed to estimate the dust coverage fraction on a PV panel surface. The dust coverage fraction was implemented in predicting the output power of the PV module, as the surface of the PV panel that is covered with the accumulated dust attenuates the energy conversion of the PV cells, while the uncovered fraction was considered a perfect energy convertor. The steady-state solution of the model provides fair agreement with the experimental results. The effect of the wind velocity on the dust coverage fraction of three types of dust (graphene, silica, and natural dust) was studied, and the results revealed that the saltation effect was induced at high wind velocity (4 m/s) for silica and natural dust, forming an opaque layer of dust. This dense (opaque) layer of dust resulted in a lower output power of the PV module in comparison to the low wind velocity (2 m/s). The effect of the dust particle size on the dust coverage fraction on the surface of a tilted PV module was also investigated, and it shows that increasing the particle size resulted in reducing the dust coverage fraction as the slipping force (surface-parallel force) is directly proportional to both particle size and tilt angle. The model successfully relates the output power of a PV module to the dust particle size and the tilt angle of the module under gravity and aerodynamic (wind) effects.

The dust coverage fraction of a mixture of different particle sizes of dust is recommended for future studies to investigate the interaction between large and fine particles through the slipping of particles downward.

Author Contributions: Conceptualization, I.A.D.; Methodology, M.A.A.M.Z.; Validation, M.F.F.; Formal analysis, A.A.A.; Data curation, M.F.F.; Writing—original draft, I.A.D.; Writing—review & editing, M.A.A.M.Z.; Supervision, M.A.A.M.Z. All authors have read and agreed to the published version of the manuscript.

Funding: This research work was funded by Universiti Kebangsaan Malaysia under Geran Universiti Penyelidikan grant number (GUP-2022-024).

Conflicts of Interest: The authors declare no conflict of interest.

Nomenclature

Symbol	Description
F_S	Slipping force (N)
F_R	Retarding force (N)
F_g	Particle weight (N)
F_{gn}	Weight normal force (N)
F_{gs}	Weight parallel force (N)
F_L	Wind lift force (N)
F_{Ln}	Lift normal force (N)
F_{Lr}	Lift parallel force (N)
F_d	Wind drag force (N)
F_{dn}	Drag normal force (N)
F_{dr}	Drag parallel force (N)
F_{vander}	Van der Waals force (N)
$F_{eletrostatic}$	Electrostatic force (N)
h_w	Lifshitz constant (eV), a measure of the maximum rate of change of a function in a region over which the function is defined
d	Particle diameter (μm)
Z_0	Average distance between particle and surface (m)
ε	Surface dust coverage fraction (area covered by dust particles relative to the total solar panel surface)
ϕ	Solar zenith angle (degrees)
$R(\omega,\theta)$	Reflectance of the cell at wavelength ω and incident angle θ
γ	Average transmission of a single dust layer
$n1$	Refractive index of air
n_ω	Real part of the refractive index of silicon at wavelength ω

R_S	Reflectance of s-polarized light
F_{eli}	Electrostatic image force (N)
Q_{dust}	Particle charge (C)
F_{eld}	Electrostatic double layer force (N)
U	Contact potential difference (V)
E	Permittivity of free space
F_{elf}	Electrostatic field force (N)
σ	Surface charge density (C/m^2)
m	Particle mass (gm)
g	Gravitational force (m/s^2)
β	Tilt angle (degrees)
k_l	Lift coefficient
k_d	Drag coefficient
ρ	Particle density (kg/m^3)
u_s	Surface friction velocity (m/s)
τ	Shear stress at boundary layer (N/m^2)
ρ_α	Air density (kg/m^3)
θ	Incident angle (degrees)
$I(\omega)$	Solar irradiance (W/m^2.nm)
$F(\theta,\beta)$	Absorption efficiency at incident angle θ and tilt angle β
ar	Angular loss coefficient
$n2$	Refractive index of silicon
k_ω	Imaginary part of the refractive index of silicon at wavelength ω
R_P	Reflectance of p-polarized light

References

1. Ahmed, Z.; Kazem, H.; Sopian, K. Effect of dust on photovoltaic performance: Review and research status. *Latest Trends Renew. Energy Environ. Infrom.* **2013**, *1*, 193–199.
2. Maghami, M.; Hizam, H.; Gomes, C.; Radzi, M.; Rezadad, M.; Hajighorbani, S. Power loss due to soiling on solar panel: A review. *Renew. Sust. Energy Rev.* **2016**, *59*, 1307–1316. [CrossRef]
3. Sayigh, A.; Al-Jandal, S.; Ahmed, H. Dust effect on solar flat surfaces devices in Kuwait. In *The Workshop on the Physics of Nonconventional Energy Sources and Materials Science for Energy*; ICTP: Trieste, Italy, 1985; pp. 353–367.
4. Hottel, H.; Woertz, B. Performance of flat-plate solar-heat collectors. *Trans. ASME* **1942**, *169*, 64. [CrossRef]
5. Garg, H. Effect of dirt on transparent covers in flat-plate solar energy collectors. *Sol. Energy* **1974**, *15*, 299–302. [CrossRef]
6. Salim, A.; Huraib, F.; Eugenio, N. PV power-study of system options and optimization. In Proceedings of the EC Photovoltaic Solar Conference, Florence, Italy, 9–13 May 1988; Volume 8, pp. 688–692.
7. Kazem, H.A.; Al-Bahri, S.; Al-Badi, S.; Al-Mahkladi, H.; Al-Waeli, A.H.A. Dust Effect on the Performance of Photovoltaic. In *Advanced Materials Research*; Trans Tech Publications: Stafa-Zurich, Switzerland, 2014; Volume 875.
8. Kaldellis, J.; Kapsali, M. Simulating the dust effect on the energy performance of photovoltaic generators based on experimental measurements. *Energy* **2011**, *36*, 5154–5161. [CrossRef]
9. He, G.; Zhou, C.; Li, Z. Review of Self-Cleaning Method for Solar Cell Array. *Proc. Eng.* **2011**, *16*, 640–645. [CrossRef]
10. Kawamoto, H.; Shibata, T. Electrostatic cleaning system for removal of sand from solar panels. *J. Electrost.* **2015**, *73*, 65–70. [CrossRef]
11. Kazem, H.A.; Chaichan, M.T.; Al-Waeli, A.H.; Sopian, K. A review of dust accumulation and cleaning methods for solar photovoltaic systems. *J. Clean. Prod.* **2020**, *276*, 123187. [CrossRef]
12. Williams, R.B.; Tanimoto, R.; Simonyan, A.; Fuerstenau, S. Vibration Characterization of Self-Cleaning Solar Panels with Piezoceramic Actuation. In Proceedings of the 48th AIAA/ASME/ASCE/AHS/ASC Structures, Structural Dynamics, and Materials Conference, Honolulu, HI, USA, 22–26 April 2007. [CrossRef]
13. Taha, H.M.; Hameed, S. Optimization of Tilt Angle of a PV System to Get Maximum Generated Power: A Case Study. *Kurd. J. Appl. Res.* **2020**, *5*, 2. [CrossRef]
14. Al-Waeli, A.H.; Sopian, K.; Kazem, H.A.; Chaichan, M.T. Photovoltaic/Thermal (PV/T) systems: Status and future prospects. *Renew. Sustain. Energy Rev.* **2017**, *77*, 109–130. [CrossRef]
15. Benatiallah, A.; Ali, A.M.; Abidi, F.; Benatiallah, D.; Harrouz, A.; Mansouri, I. Experimental Study of Dust Effect in Mult-Crystal PV Solar Module. *Int. J. Multidiscip. Sci. Eng.* **2012**, *3*, 3.
16. Chen, J.; Ma, Y.; Pang, Z. A mathematical model of global solar radiation to select the optimal shape and orientation of the greenhouses in southern China. *Sol. Energy* **2020**, *205*, 380–389. [CrossRef]

17. Lu, J.; Hajimirza, S. Optimizing sun-tracking angle for higher irradiance collection of PV panels using a particle-based dust accumulation model with gravity effect. *Sol. Energy* **2017**, *158*, 71–82. [CrossRef]
18. Goossens, D.; Van Kerschaever, E. Aeolian dust deposition on photovoltaic solar cells: The effects of wind velocity and airborne dust concentration on cell performance. *Sol. Energy* **1999**, *66*, 277–289. [CrossRef]
19. Picotti, G.; Borghesani, P.; Cholette, M.E.; Manzolini, G. Soiling of solar collectors—Modelling approaches for airborne dust and its interactions with surfaces. *Renew. Sustain. Energy Rev.* **2018**, *81*, 2343–2357. [CrossRef]
20. Asl Gholami, A.; Khazaee, I.; Eslami, S.; Zandi, M.; Akrami, E. Experimental investigation of dust deposition effects on photo-voltaic output performance. *Sol. Energy* **2018**, *159*, 346–352. [CrossRef]
21. Mekhilef, S.; Saidur, R.; Kamalisarvestan, M. Effect of dust, humidity and air velocity on efficiency of photovoltaic cell. *Renew. Sustain. Energy Rev.* **2012**, *16*, 2920–2925. [CrossRef]
22. Hee, J.Y.; Kumar, L.V.; Danner, A.J.; Yang, H.; Bhatia, C.S. The effect of dust on transmission and self-cleaning property of solar panel. *Energy Procedia* **2012**, *15*, 421–427. [CrossRef]
23. Jiang, Y.; Lu, L.; Ferro, A.R.; Ahmadi, G. Analyzing wind cleaning process on the accumulated dust on solar photovoltaic (PV) modules on flat surfaces. *Sol. Energy* **2018**, *159*, 1031–1036. [CrossRef]
24. Tominaga, Y.; Akabayashi, S.I.; Kitahara, T.; Arinami, Y. Air flow around isolated gable-roof buildings with different roof pitches: Wind tunnel experiments and CFD simulations. *Build. Environ.* **2015**, *84*, 204–213. [CrossRef]
25. Hamid, N.F.A.; Zainuri, M.A.A.M.; Hussain, A. Self-Charging Technique for DC-Link Capacitor Voltage Control: A Review. In Proceedings of the International Conference on Electrical Engineering and Informatics (ICEEI), Kuala Terengganu, Malaysia, 12–13 October 2021; pp. 1–6. [CrossRef]
26. Katzan, C.; Edwards, J. *Lunar Dust Transport and Potential Interactions with Power System Components*; NASA Contractor Report; NASA: Greenbelt, MD, USA, 1991; p. 4404.
27. Zang, J.; Wang, Y. Analysis of computation model of particle deposition on transmittance for photovoltaic panels. *Energy Proc.* **2011**, *12*, 554–559. [CrossRef]
28. Al-Hasan, A. A new correlation for direct beam solar radiation received by photovoltaic panel with sand dust accumulated on its surface. *Sol. Energy* **1998**, *63*, 323–333. [CrossRef]
29. Wang, J.; Gong, H.; Zou, Z. Modeling of dust deposition affecting transmittance of PV modules. *J. Clean Energy Technol.* **2017**, *5*, 217–221. [CrossRef]
30. Tanabe, K. Modeling of airborne dust accumulation on solar cells at the Martian surface. *Acta Astronaut.* **2008**, *62*, 683–685. [CrossRef]
31. Guo, B.; Javed, W.; Figgis, B.; Mirza, T. Effect of dust and weather conditions on photovoltaic performance in Doha, Qatar. In Proceedings of the 2015 First Workshop on Smart Grid and Renewable Energy, Doha, Qatar, 22–23 March 2015; Volume 62, pp. 1–6.
32. Lai, A.C.; Nazaroff, W.W. Modeling indoor particle deposition from turbulent flow onto smooth surfaces. *J. Aerosol Sci.* **2000**, *31*, 463–476. [CrossRef]
33. Hussein, T.; Smolik, J.; Kerminen, V.; Kulmala, M. Modeling dry deposition of aerosol particles onto rough surfaces. *Aerosol Sci. Technol.* **2012**, *46*, 44–59. [CrossRef]
34. Zhao, B.; Wu, J. Modeling particle deposition from fully developed turbulent flow in ventilation duct. *Atmos. Environ.* **2006**, *40*, 457–466. [CrossRef]
35. Reeks, M.; Hall, D. Kinetic models for particle resuspension in turbulent flows: Theory and measurement. *J. Aerosol Sci.* **2001**, *32*, 1–31. [CrossRef]
36. Available online: https://en.wikipedia.org/wiki/Van_der_Waals_force (accessed on 1 August 2023).
37. Jiang, C.S.; Moutinho, H.R.; To, B.; Xiao, C.; Simpson, L.J.; Al-Jassim, M.M. Decay of Electrostatic Force of Dust Particles on Photovoltaic Modules. In Proceedings of the IEEE 46th Photovoltaic Specialists Conference (PVSC), Chicago, IL, USA, 16–21 June 2019. [CrossRef]
38. Fryrear, D.W.; Stout, J.E.; Hagen, L.J.; Vories, E.D. Wind erosion: Field measurement and analysis. *Trans. ASAE* **1991**, *34*, 155–0160. [CrossRef]
39. Rentsch, S.; Pericet-Camara, R.; Papastavrou, G.; Borkovec, M. Probing the validity of the Derjaguin approximation for heterogeneous colloidal particles. *Phys. Chem. Chem. Phys.* **2006**, *8*, 2531–2538. [CrossRef] [PubMed]
40. Meng, G.; Gao, D.; Wang, S.; Xin, Y.; Zheng, H. Mechanics modeling of dust particle on solar panel surface in desert environment. *Trans. Chin. Soc. Agric. Eng.* **2014**, *30*, 221–229. [CrossRef]
41. Behrens, S.; Grier, D. The charge of glass and silica surfaces. *J. Chem. Phys.* **2001**, *115*, 6716–6721. [CrossRef]
42. Liu, C.N.; Chien, C.L.; Lo, C.C.; Lin, G.Y.; Chen, S.C.; Tsai, C.J. Drag Coefficient of a Spherical Particle Attached on the Flat Surface. *Aerosol Air Qual. Res.* **2011**, *11*, 482–486. [CrossRef]
43. Ekanayake, N.; Berry, J.; Harvie, D. Lift and drag forces acting on a particle moving in the presence of slip and shear near a wall. *J. Fluid Mech.* **2021**, *915*, A103. [CrossRef]
44. Alsalihi, A.M.; Abdulatif, S.H. Analysis Global and Ultraviolet Radiation in Baghdad City, Iraq. *J. Nat. Sci. Res.* **2016**, *6*, 22.
45. Konyu, M.; Ketjoy, N.; Sirisamphanwong, C. Effect of dust on the solar spectrum and electricity generation of a photovoltaic module, IET Renew. *Power Gener.* **2020**, *14*, 2759–2764. [CrossRef]

46. Bezerra, M.A.; Santelli, R.E.; Oliveira, E.P.; Villar, L.S.; Escaleira, L.A. Response surface methodology (RSM) as a tool for optimization in analytical chemistry. *Talanta* **2008**, *76*, 965–977. [CrossRef]
47. Kiran, B.; Kaushik, A.; Kaushik, C.P. Response surface methodological approach for optimizing removal of Cr (VI) from aqueous solution using immobilized cyanobacterium. *Chem. Eng. J.* **2007**, *126*, 147–153. [CrossRef]